REPRINTED FROM THE

Proceedings

OF THE NINTH

Midwestern Mechanics Conference

(A MIDWESTERN MECHANICS CONFERENCE PUBLICATION)

HELD AT THE UNIVERSITY OF WISCONSIN,
MADISON, WISCONSIN, AUGUST 16-18, 1965

ELASTOPLASTICITY AND THE ATTENUATION OF SHOCK WAVES

JOHN O. ERKMAN
Stanford Research Institute, Menlo Park, California

GEORGE E. DUVALL
Washington State University, Pullman, Washington

Calculations have been performed for the case of a thin projectile striking a semi-infinite target. Because the projectile is considered to be infinite in extent in directions perpendicular to its direction of travel, the resulting flow is one-dimensional in the strain. It is assumed that stresses and strains are related by elastoplastic relations. Work of other authors has been extended so that (1) the shear modulus depends on the magnitude of the hydrostatic compression; (2) the yield is increased as the hydrostatic pressure is increased; (3) the artificial viscosity method is used for solving the flow equations. Poisson's ratio is assumed to be a constant. Comparison of the calculated results with experimental results gives strong support to the assumptions that both aluminum and copper yield elastoplastically when the maximum stress is about 0.1 megabars. No difficulties are found in applying the artificial viscosity method developed by von Neumann and Richtmyer to problems involving elastoplastic flow.

I. Introduction

The mechanics of attenuation of stress waves in elastoplastic solids has been the subject of extensive theoretical and experimental investigations during the last twenty-five years. Most of these studies have been directed toward the understanding of wave propagation in rods and, after the first blush of success reported by von Karman and Taylor, successful correlations of calculations and measurements have been few. At least part of this failure has been due to the essentially two-dimensional character of wave propagation on a bar; other deviations have been widely attributed to the dependence of yield point and plastic moduli on strain rates.

In recent years it has become possible to produce well-controlled plane waves in solids by means of explosive or high velocity impact. During the same period techniques for precisely measuring the waves so produced have been developed, and meaningful comparisons between measurements and theoretical calculations under conditions of true uniaxial strain have become possible. During this same period the development of high speed computing machines has made it a relatively simple matter to systematically alter the constitutive relations used for wave calculations and so to approach a theoretical model that agrees arbitrarily well with experimental measurements. It was toward such a comparison that work reported here was directed.

The work was performed in a study of the attenuation of shock waves in aluminum and copper. The amplitude of the stress carried by the shock waves was about 0.1 megabar (10^{11} dynes/cm^2, or approximately 10^5 atmospheres). Measurements were made of the free-surface velocities of targets that had been hit by projectiles in the form of 1/8 inch thick aluminum plates that had been accelerated to a velocity of about 0.125 cm/μsec by high explosives. The use of targets of progressively greater thickness gave information on the attenuation of the shock in the material being studied.

The results of these experiments are compared with the results of calculations based on an elastoplastic model for the relation of stress to strain (or stress to volume) and a fluid model.

The compression in a uniform shock wave traveling through an elastoplastic medium can be adequately described with conventional analysis supplemented by relatively simple numerical computations based on the theory of characteristics. When the shock wave is nonuniform,

wave interactions complicate the calculations, as do the presence of interfaces between materials having different acoustic impedances. For such reasons, the method of characteristics is not suitable in many situations for which numerical solutions are desired. An alternative is available in the form of the method of von Neumann and Richtmyer [1]. Boundaries, including free surfaces, are readily accommodated by this method and its application to the flow in an elastoplastic medium is straightforward. A detailed comparison of the relative advantages of the theory of characteristics and the method of von Neumann and Richtmyer (hereafter called the Q-method) in different problems is given by Fife, Eng, and Young [2] for the simpler case of wave propagation in a fluid.

The Q-method consists of using finite difference equations based on increments in real space and time to replace the differential equations that describe the flow, and of smoothing discontinuities through introduction of an artificial viscosity. For one-dimensional flow, the equations of continuity and motion in Lagrangian coordinates are

$$\rho_0 \frac{\partial V}{\partial t} = \frac{\partial u}{\partial x} \tag{1}$$

$$\rho_0 \frac{\partial u}{\partial t} = -\frac{\partial (p_x + Q)}{\partial x}, \tag{2}$$

where u is particle velocity, V is specific volume, t is time, x is Lagrange space coordinate, ρ_0 is density of the undisturbed medium, and p_x is compressive stress in the x direction. Q is the artificial viscosity. The particular form for Q used in the present case is

$$Q = -\frac{(C_q \Delta x)^2}{V} \frac{\partial u}{\partial x} \left| \frac{\partial u}{\partial x} \right|. \tag{3}$$

This form for Q satisfies the following conditions:

a. It eliminates discontinuities in the flow field;

b. The thickness of the shock layer is the order of the space increment, Δx, used in the computation;

c. The effects of Q outside the shock layers are negligible;

d. The Rankine-Hugoniot equations hold if gradients outside the shock layer are small.

The use of this method when p_x and V are related by an elastoplastic model has caused no problems with instabilities in the calculations.

II. The Elastoplastic Relation Between Stress and Strain

Earlier work on the theory of plane wave propagation in elastoplastic materials was done by White and Griffis [3], Wood [4], and Morland [5]. Their numerical methods were inadequate for generalization to finite amplitude waves, however, and this work may be regarded as an extension of theirs. At present only one-dimensional strain is considered, and the direction of propagation is taken to be the x-axis; stresses and strains without subscripts relate to that direction. Figure 1 shows the stress-strain relations in a cycle of one-dimensional compression starting at $p_x = \eta = 0$. We can always write the identity

$$dp_x = d\bar{p} + 4/3\, d\tau, \tag{4}$$

where $\bar{p}$ is mean compressive stress, p_x is compressive stress in the direction of propagation, and $d\tau = (dp_x - dp_y)/2$ is maximum resolved shear stress. In the plastic state, $d\tau = 0$ except for strain hardening. For both the Tresca and the von Mises yield conditions in this geometry, the maximum value of τ is determined by the yield stress, $Y = 2\tau$. Equation (4) is to be specialized for the curve segments *ba*, *ae*, *ef*, and *fb* of Fig. 1

Along *ba:*

The material is behaving elastically, $\tau < Y/2$, and so

$$dp_x = (K + 4\mu/3) d\epsilon_x = 3d\bar{p}\,(1 - \nu)/(1 + \nu), \tag{5}$$

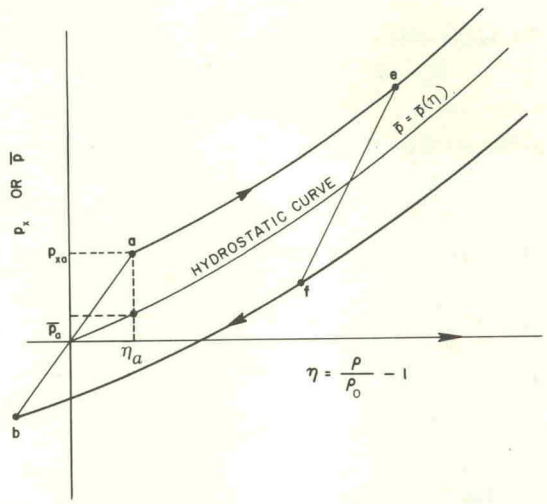

Fig. 1. Elastoplastic Equation of State

where K is bulk modulus, μ is rigidly modulus, ν is Poisson's ratio, $d\epsilon_x = d\rho/\rho$ is incremental strain in the x-direction and ρ is density. For ν = const., which is assumed throughout the following, Eq. (5) can be integrated directly:

$$p_x = 3\bar{p}(1-\nu)/(1+\nu). \tag{6}$$

Since strain is uniaxial,

$$dp_y = (K - 2\mu/3)\, d\epsilon_x , \tag{7}$$

and the incremental change in τ is

$$d\tau = (dp_x - dp_y)/2 = 3d\bar{p}(1-2\nu)/2(1+\nu) \tag{8}$$

or

$$\tau = 3\bar{p}(1-2\nu)/2(1+\nu). \tag{9}$$

At *a:*

This is the initial yield point, so

$$Y_a = 2\tau_a = 3\bar{p}_a(1-2\nu)/(1+\nu). \tag{10}$$

Along *ae:*

Equation (4) is integrated to obtain

$$p_x - p_{xa} = \bar{p} - \bar{p}_a + \frac{2}{3}(Y - Y_a). \tag{11}$$

At *e:*

As unloading begins, yield ceases, and

$$Y = Y_e. \tag{12}$$

Along *ef:*

This is the unloading phase; τ diminishes and changes sign, and the material once again behaves elastically. Equation (5) integrates to

$$p_{xe} - p_x = 3(1-\nu)(\bar{p}_e - \bar{p})/(1+\nu).$$

The integral of Eq. (8) is

$$Y_e - 2\tau = 3(\bar{p}_e - \bar{p})(1-2\nu)/(1+\nu).$$

Combining this with Eq. (12) yields

$$Y_e - 2\tau = (p_{xe} - p_x)(1 - 2\nu)/(1 - \nu) \tag{13}$$

At *f:*

This is the unloading yield point;

$$p_y - p_x = Y_f = -2\tau_f \tag{14}$$

and from Eq. (13),

$$Y_e + Y_f = (p_{xe} - p_{xf})(1 - 2\nu)/(1 - \nu)$$

$$p_{xe} - p_{xf} = \frac{1 - \nu}{1 - 2\nu}(Y_e + Y_f). \tag{15}$$

In the special case $Y_f = Y_e$, $\nu = 1/3$,

$$p_{xe} - p_{xf} = 4Y_e.$$

Along *fb:*

Here we have the integral of Eq. (4):

$$p_x - p_{xf} = \bar{p} - \bar{p}_f - \frac{2}{3}(Y - Y_f). \tag{16}$$

At *b:*

The resolved shear stress, calculated elastically, is equal to half the yield stress:

$$Y_b = 2\tau_b = 3\bar{p}_b(1 - 2\nu)/(1 + \nu). \tag{17}$$

Equations (5) through (17) provide means for calculating the stress-strain cycle of Fig. 1 if $\bar{p}(\rho)$, $Y(\bar{p})$, and ν are known. The extent to which ν may vary during such a cycle is presently unknown.

The value of the yield strength is assumed to vary with the pressure according to the relation

$$Y = Y_0 + M(\bar{p} - \bar{p}_a) \quad . \tag{18}$$

The mean pressure is assumed to be related to the density by the expression

$$\bar{p} = A\eta + B\eta^2 + C\eta^3 \tag{19}$$

where $\eta = (\rho/\rho_0) - 1$ and ρ_0 is density at $\bar{p} = 0$. The sound speed is

$$c = \sqrt{dp_x/d\rho} = [-3V^2(1 - \nu)(d\bar{p}/dV)/(1 + \nu)]^{1/2} \tag{20}$$

Sound speed is assumed constant, $c = c_0$, along *ba* of Fig. 1. Integrating Eq. (20) under this assumption yields

$$\bar{p} = [c_0^2(1 + \nu)/3(1 - \nu)](V^{-1} - V_0^{-1}). \tag{21}$$

Then, at *a,*

$$\eta_a = 3\bar{p}_a V_0(1 - \nu)/c_0^2(1 + \nu). \tag{22}$$

Sound speed on the segments *ae, fb* of Fig. 1 is defined by the slopes of the curves shown:

$$c_p^2 = dp_x/d\rho = d\bar{p}/d\rho \pm \frac{2}{3} dY/d\rho. \tag{23}$$

The values of the coefficients in Eq. (19) are obtained by assuming that Hugoniot equation of state data lie on the upper curve of Fig. 1. Values of Y_0 and M must then be assumed, see Eq. (18). The value of Y_0 corresponds to that obtained statically, and the value of M is esti-

mated from impact experiments. Handbook values are used for Poisson's ratio, ν, and for the elastic wave velocity, c_0. These data make it possible to extract a hydrostat from the Hugoniot data, from which the coefficients in Eq. (19) are obtained by the method of least squares. Values of the parameters are given in Table 1 for aluminum and copper.

TABLE I

Parameters for the Elastoplastic Stress-Strain Relation

Material	μ_a	Y_0^*	M	A^*	B^*	C^*	C_0^{**}	ρ_0^{***}
Aluminum	0.00438	0.0025	0.055	0.755	1.29	1.2	0.640	2.785
Copper	0.00062	0.0007	0.031	1.495	0.55	11.8	0.503	8.936

*Units are megabars (10^{12} dynes/cm^2).
**Units are cm/μsec.
***Units are g/cc.

III. Results of Calculations

The waves generated by impact on a target of a strain-free projectile plate of thickness d are represented in Fig. 2. The figure represents a case in which the material exhibits no rigidity and entropy effects are negligible, i.e., the material is a particularly simple fluid. Coordinates in the figure are distance, x, and time, t. Trajectories of the front and back of the projectile are shown before impact as sloping, parallel lines. After impact, shocks propagate into both the target and the projectile. The backward-facing shock is reflected at the free surface of the projectile as a rarefaction centered at the point B in the figure, and is represented as being composed of four waves. These waves propagate forward through the projectile and cross the interface into the target. If the material in the target differs from that of the projectile, each wave is partially reflected at the interface, $ACFH$ . . . . The reflected waves interact with the incident waves (points D, E, and G in the figure). When both the projectile and the target materials are identical, the reflected waves have zero strength and the paths of waves

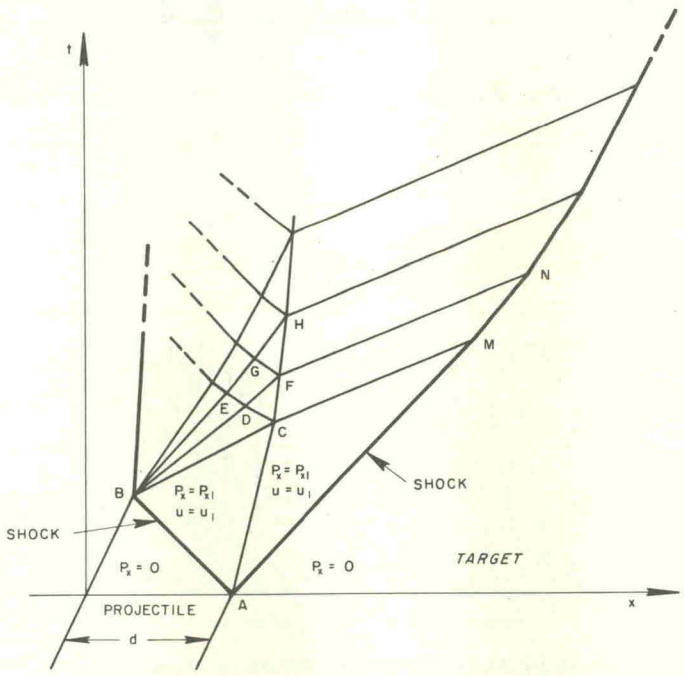

Fig. 2. Physical Plane for Plate Impact Experiment

from point B to their intersection with the shock front are straight lines. The first wave overtakes the shock at point M and reduces the pressure in the shock front. Precise measurement of the distance required for this interaction to occur would help in deciding whether the head of the rarefaction wave represented by BCM in the figure travels at hydrodynamic velocity or at elastic velocity.

The flow induced in a projectile and a target has been calculated by Fowles [6]. In the calculations it was assumed that entropy effects were negligible so that pressure was a function of volume only, and the velocity of the waves was assumed to be hydrodynamic. The calculations give, for example, the shape of the wave at any time, as shown in Fig. 3. The ordinate in the figure is the pressure, and the abscissa is the distance measured from the back side of the projectile at the instant it first contacts the target. Each wave profile is labeled with the time elapsed since the flying plate collided with the target. The projectile in this example was about 3 mm thick and had a velocity of 0.163 cm/μsec. Note that at a time of 3 μsec the wave has a flat top. This wave decays to a triangular wave of smaller amplitude but of greater duration. The decrease in amplitude of the wave is called attenuation in this paper.

Some results obtained by using the Q-method and the elastoplastic relations are shown in Fig. 4. These results are in the form of stress profiles, that is, stress is shown as a function of the distance for different values of the time following impact. Distance is an Eulerian coordinate in this and the following figures and is obtained from the calculations. The origin of the Eulerian coordinate is the same as the origin shown in Fig. 2. Profiles are given in

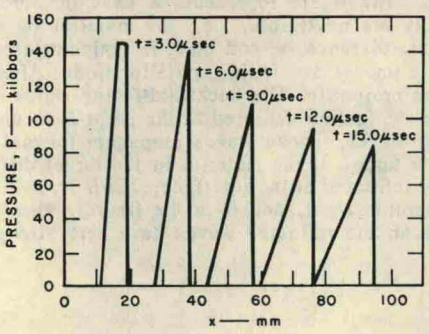

Fig. 3. Profiles of Pressure Behind Shock at Fixed Times (From Fowles)

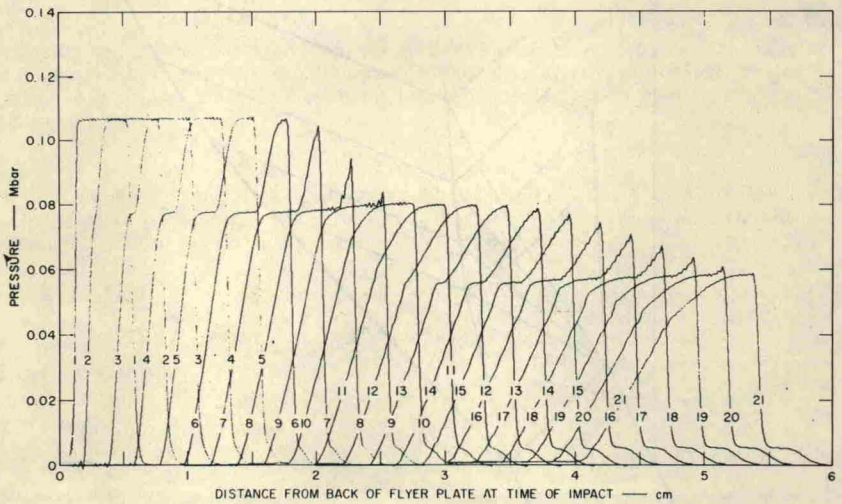

Fig. 4. Profiles of Stress for Aluminum Projectile Hitting an Aluminum Target. Projectile thickness 0.322 cm. Projectile velocity 0.125 cm/μsec.

Fig. 4 at 0.4-μsec intervals following the impact of the projectile, and the profiles are numbered sequentially. The first profile shows both the shock front in the projectile, which is 0.32 cm thick, and the shock in the target, and the top of the wave is essentially flat. The effect of the elastic relief wave is clearly shown by the profiles numbered 3 through 9. The amplitude of this relief wave is about 0.03 megabar, and the entire shock wave is reduced in amplitude, or attenuated, by 0.03 megabar in about 3.6 μsec. After the initial interaction, the profile is again relatively flat (see profile 10). The elastic relief wave is reflected from the shock front, becoming a backward-facing compression wave. This compression wave must be an elastic wave, since the region into which it propagates, marked A1 in Fig. 5, must be represented by a point on a curve such as that labeled *ef* in Fig. 1. This backward facing wave then interacts with the plastic rarefaction centered at the point *B*, Fig. 2. There results another forward facing elastic relief wave which subsequently overtakes the shock front and causes the process to be repeated. Profiles numbered 12 through 18 show this latter wave overtaking the shock front. Hence the ever-changing shapes of the pressure profiles are due to the interaction of the elastic waves with the shock front and with the following plastic relief wave as shown in part in Fig. 5.

The profiles of Fig. 6 show the effects of elastic and plastic wave interactions on the particle velocity for the same problem that was illustrated in Fig. 4. Results of the calculations can be presented more compactly by showing only the envelope of the stress profiles or of the particle velocity profiles. Such curves are shown in Fig. 7, which give the peak particle velocity as a function of the nondimensional distance x/d for both the elastoplastic model and the fluid model. For the latter, the equation of state

$$P = A\left[\left(\frac{V_0}{V}\right)^k - 1\right]$$

was used for which pairs of values of A and K were chosen to fit the Hugoniot data for the material. Three pairs of values of A and K were used in separate calculations to show the sensitivity of the calculations to the way in which the Hugoniot data were fitted. The method of characteristics was used in these calculations. Results of the fluid model show that the relief waves overtake the shock front at a greater depth in the target than do the relief waves for the elastoplastic model. That is, the shock is attenuated more rapidly by the elastic relief wave than by the relief wave in the fluid model. This observation is true for any reasonable means of evaluating the constants A and K from the Hugoniot data.

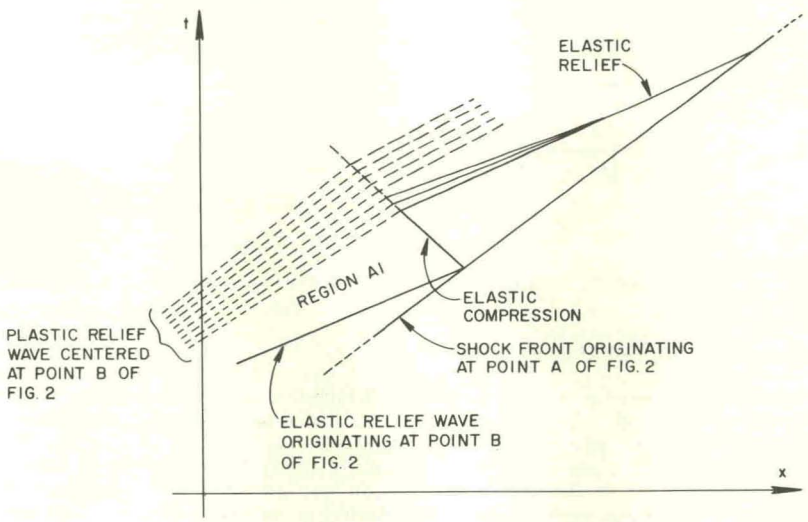

Fig. 5. Physical Plane Showing Interaction of Elastic Relief Wave and Shock Front

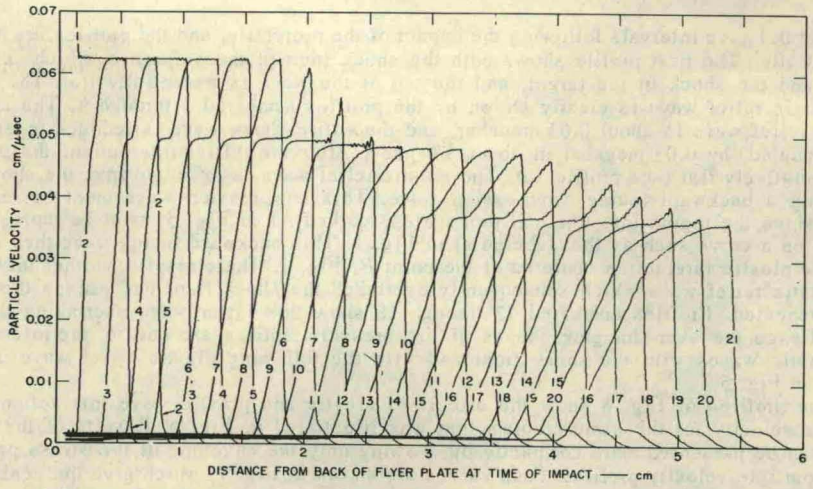

Fig. 6. Profiles of Particle Velocity for Aluminum Projectile Hitting an Aluminum Target. Projectile thickness 0.322 cm. Projectile velocity 0.125 cm/μsec.

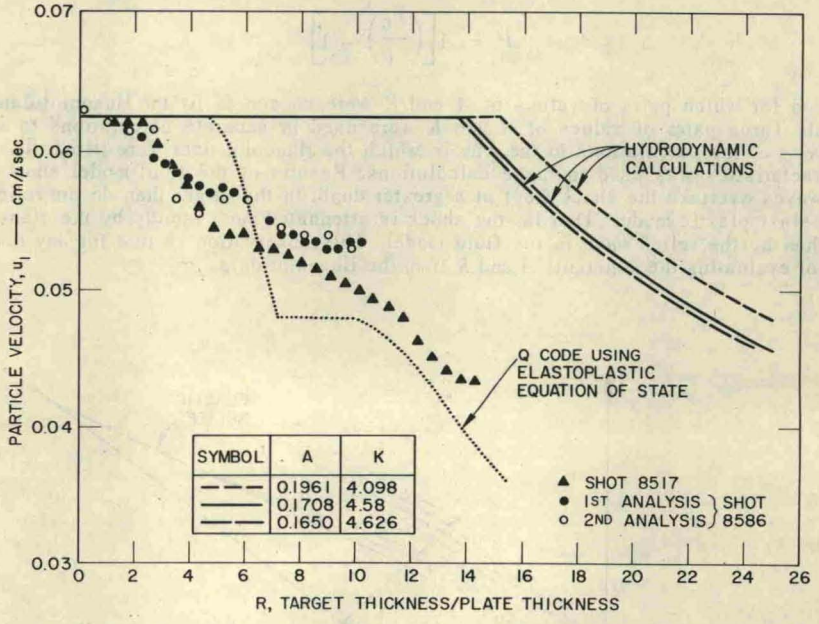

Fig. 7. Peak Particle Velocity in Aluminum Target Hit by an Aluminum Projectile

IV. Comparison with Experiment

Experiments have been performed in which 1/8-inch-thick aluminum plates have been projected at velocities of about 0.125 cm/μsec [7, 8]. In such an experiment, the observed quantity is the velocity of the free surface of the target. It has been shown that the free-surface velocity is approximately equal to twice the particle velocity behind the shock which hits the surface [9]. Although the derivation of this relation was based on the assumption of a fluid-type equation of state, the approximation is expected to be reasonably valid for the elastoplastic model. Thus, by the use of targets of different thicknesses, data can be obtained which

can be compared with the calculations. Such data are plotted in Fig. 7. It is readily apparent that the experimental data agree more closely with the results obtained by the use of the elastoplastic model than with those obtained by the use of the fluid model.

Peak particle velocity as a function of distance is shown in Fig. 8 for the case of an aluminum plate hitting a copper target. Again, the results obtained with the elastoplastic model more nearly agree with the experimental data than do the results from the fluid model. This result is obtained for all reasonable representations of the Hugoniot data of aluminum and copper, i.e., different pairs of values of the parameters A and K.

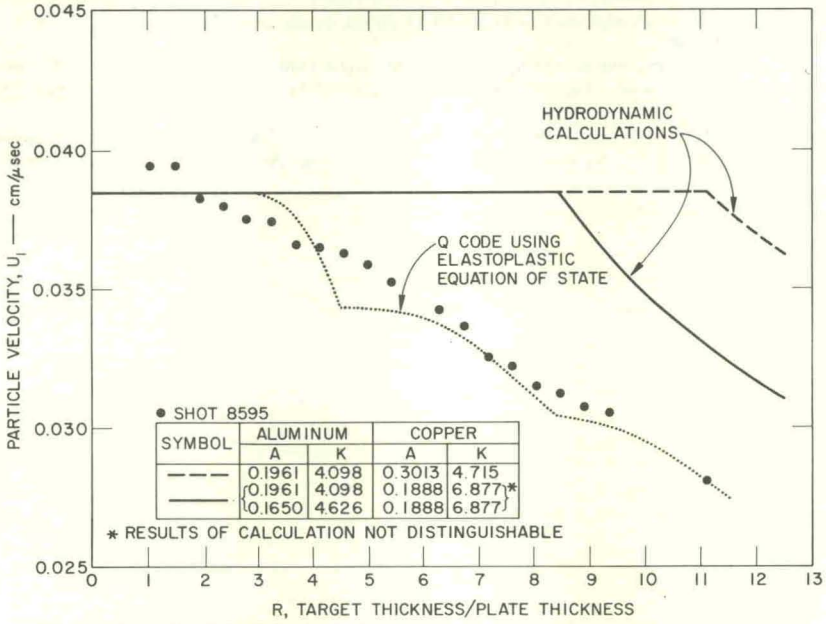

Fig. 8. Peak Particle Velocity in Copper Target Hit by an Aluminum Projectile

V. Conclusions

The numerical method for calculating shocks developed by von Neumann and Richtmyer [1] has been successfully applied to a problem involving an elastoplastic stress-strain relation. Comparison of the results of the numerical work with the results of experiments shows that elastoplastic behavior of aluminum and copper is required to account for the observed rapid attenuation of shock waves. Present results are valid for stresses up to 0.1 megabar in aluminum and up to 0.15 megabar in copper.

Acknowledgment

This research was initiated by the Air Force Special Weapons Center under Contract No. AF 29(601)–6040. It was also partially supported by the Advanced Research Projects Agency, and the Air Force Office of Scientific Research under Contract No. AF 49(638)–1086, and by the Defense Atomic Support Agency under Contract No. DA–49–146–XZ–095.

References

1. von Neumann, J., and R. D. Richtmyer, A method for the numerical calculation of hydrodynamic shocks, *J. Appl. Phys.*, Vol. 21, 1950, pp. 232–237.
2. Fife, I. M., R. C. Eng, and D. M. Young, On the numerical solution of the hydrodynamic equations, *SIAM Review*, Vol. 3, 1961, pp. 298–308.

3. White, M. P. and L. Griffis, The propagation of plasticity in uniaxial compression, *J. Appl. Mech.*, Reprint–Paper No. 48, APM–17, 1948.
4. Wood, D. S., On longitudinal waves of elastic-plastic strain in solids, *J. Appl. Mech.*, Vol. 19, 1952, p. 521.
5. Morland, L. W., The propagation of plane irrotational waves through an elastoplastic medium, *Phil. Trans. Roy. Soc.*, London, Ser. 251, 1959, pp. 341–383.
6. Fowles, G. R., Attenuation of the shock wave produced in a solid by a flying plate, *J. Appl. Phys.*, Vol. 31, 1960, pp. 655–661.
7. Curran, D. R., Nonhydrodynamic attenuation of shock waves in aluminum, *J. Appl. Phys.*, Vol. 34, 1963, pp. 2677–2685.
8. Erkman, J. O., Hydrodynamic theory and high pressure flow in solids, Technical Summary Report, No. 2, Stanford Res. Inst., Proj. No. PGU–3712, Stanford Research Institute, Menlo Park, California, 1962.
9. Rice, M. H., R. G. McQueen, and M. Walsh, Compression of solids by strong compression waves, *Solid State Physics*, Vol. 6, F. Seitz and D. Turnbull, eds., Academic Press, N. Y., 1958, pp. 1–63.